Journal of Water Process Engineering 71 (2025) 107368

Contents lists available at ScienceDirect

Journal of Water Process Engineering

journal homepage: www.elsevier.com/locate/jwpe

Superhydrophobic northern tooth-like ZnO nanosheets on stainless steel mesh for oil-water separation

Tanuja A. Ekunde [a], Pradip P. Gaikwad [a], Rajaram S. Sutar [b], Shrutika S. Kshirsagar [a], Rutuja A. Ekunde [a], Arvind M. Yelpale [c], Xuesong Huang [d], Viswanathan S. Saji [e], Shanhu Liu [b,*], Sanjay S. Latthe [a,b,**]

[a] Self-cleaning Research Laboratory, Department of Physics, Vivekanand College (Autonomous), Affiliated to Shivaji University, Kolhapur 416 003, Maharashtra, India
[b] College of Chemistry and Molecular Science, Henan University, Kaifeng 475004, China
[c] Department of Physics, Shahajiraje Mahavidyalaya, Khatav, Satara 415505, Affiliated to Shivaji University, Kolhapur, India
[d] Institute of Petroleum Engineering Technology, Sinopec Zhongyuan Oilfield, Puyang 457001, China
[e] Interdisciplinary Research Center for Advanced Materials, King Fahd University of Petroleum & Minerals, Dhahran 31261, Saudi Arabia

ARTICLE INFO

Editor: Ludovic F. Dumée

Keywords:
Superhydrophobic mesh
ZnO nanosheets
Oil-water separation
Northern tooth
Stainless steel mesh

ABSTRACT

2D nanosheets, with their unique shape, possess an increased surface area and active sites for interactions with liquid molecules, making them highly effective absorbents. This study introduces a novel hierarchical Northern Tooth-like zinc oxide (ZnO) nanosheet growth on stainless steel (SS) mesh. The growth is achieved via heterogeneous nucleation during immersion in alcoholic solution of zinc acetate dihydrate and diethanolamine, which was followed by a stearic acid (STA) modification. The process of zinc ions (Zn^{2+}) hydrolysis and anisotropic growth on the SS mesh, facilitated by its surface roughness and controlled reaction conditions, leads to the formation of tooth-like ZnO nanosheets. STA, by bonding its carboxyl groups with Zn^{2+} ions, reduces surface energy, promotes self-assembly, and stabilizes nanosheet morphology. The coated SS mesh showed superhydrophobicity with a water contact angle (WCA) of 162 ± 2° and a sliding angle (SA) of 3°. SEM confirmed Northern Tooth-like ZnO nanosheet growth on SS mesh. The superhydrophobic SS mesh achieved 99 % separation for petrol and 92 % for vegetable oil. The permeation fluxes were recorded at 700 ± 50 L/m^2·h for the petrol and 135 ± 50 L/m^2·h for the vegetable oil. SS mesh remained superhydrophobic after undergoing 70 cycles of adhesive tape peeling tests, 20 cycles of sandpaper abrasion tests, and multiple torsion, bending, and folding motions. It also withstood exposure to heat and both alkaline and acidic environments. Furthermore, the mesh demonstrated a remarkable self-cleaning ability. The proposed formulation for creating a superhydrophobic mesh is promising for oil-water separation applications.

1. Introduction

Frequent oil spills and untreated industrial and sanitary wastewater pose significant environmental challenge worldwide. These pollutants contaminate water sources and threaten aquatic life and human health. Various methods have been developed to address the issue of oil-water contamination, each with its own operational principles and limitations [1–4]. Additionally, many of these methods require considerable time and resources, leading to increased operational costs and the potential generation of secondary pollutants, which can worsen environmental problems rather than solving them. Given these challenges, there is an urgent need for the development of low-cost, high-performance oil-water separation technology with superhydrophobic/superoleophilic properties. Such technology could improve the efficiency of oily wastewater treatment by enhancing the separation process, providing a more effective and environmentally friendly solution to oil-contaminated water.

In recent decades, there has been growing interest in the synthesis and utilization of superhydrophobic/superoleophilic meshes [5], membranes [6], aerogel [7], sponges [8], cotton fabrics [9], and other

* Correspondence to: S. Liu, College of Chemistry and Molecular Science, Henan University, Kaifeng 475004, China.
** Correspondence to: S.S. Latthe, Self-cleaning Research Laboratory, Department of Physics, Vivekanand College (Autonomous), Affiliated to Shivaji University, Kolhapur 416 003, Maharashtra, India.
E-mail addresses: liushanhu@vip.henu.edu.cn (S. Liu), latthes@gmail.com (S.S. Latthe).

https://doi.org/10.1016/j.jwpe.2025.107368
Received 11 January 2025; Received in revised form 17 February 2025; Accepted 24 February 2025

porous materials [10] for separating oil-water mixtures. These materials possess excellent wettability and porosity, which enhance oil absorption while repelling water. Among these, metal meshes have gained significant attention due to their outstanding filtration, durability, reusability, and suitability for large-scale industrial applications. Moreover, metal meshes are highly flexible, allowing them to be shaped into various forms and configurations, thereby increasing their effectiveness in different separation scenarios. Various types of metal meshes, such as those made from nickel [11], copper [12], and stainless steel (SS) [13], have been successfully used in oil-water separation. Several technologies have been developed to create superhydrophobic (strongly repels water) and superoleophilic (strongly attracts oil) surfaces on SS mesh. One common method combines inorganic nanostructured materials with polymers to improve the physical and functional properties of the mesh [14]. Another effective approach involves creating a rough texture through etching or nanostructured growth, followed by applying low surface energy chemicals [15–17].

Zinc oxide (ZnO) is an eco-friendly, photosensitive, water-insoluble transition metal oxide with high thermal conductivity and low thermal expansion. Notably, ZnO can be grown into different nanostructure forms such as nanorods [18], nanopillars [19], nanoflowers [20], nanoparticles [21,22], nanosheets [23], and nanowires on different substrates, each with unique characteristics. Xiong et al. have grown ZnO nanopillars on polyethylene terephthalate (PET) nanofibers to attain a hierarchical surface structure [24]. After a hydrophobic modification, the ZnO nanopillar-containing PET nanofiber membrane was utilized to treat oil-contaminated water. Wang et al. have made growth of ZnO nanoneedles onto surface-sulfonated poly(ether-ether-ketone) (PEEK) felt using UV/ozone cleaning followed by hydrothermal synthesis [25]. The modified felt demonstrated improved anti-fouling performance in the separation of oil-water mixtures. Wei et al. have developed ZnO nanoflowers of various sizes on SiC grains, forming tunable hierarchical structures on the SiC membrane surface [26]. Bai et al. grew rod-shaped ZnO nanostructures on electrospun carbon nanofiber membranes through a hydrothermal method, and then modified them with 1H, 1H, 2H, 2H-perfluorooctyltriethoxysilane to achieve superhydrophobic and superoleophilic properties for treating oil-contaminated water [27]. Eventually, the innovations in the growth of ZnO nanostructures on SS mesh could enable tailored properties that could significantly improve its performance in practical applications.

We report the Northern Tooth-like growth of ZnO nanosheets on SS mesh for oil-water separation. We introduce a novel approach to controlling surface wettability by synthesizing ZnO nanosheets and modifying them with stearic acid (STA). The carboxyl groups of STA bond with Zn^{2+} ions, anchoring hydrophobic chains, while esterification with ZnO's hydroxyl groups reduces surface energy, ensuring durable hydrophobicity. The northern tooth-like 2D ZnO nanosheets may garner significant attention due to their unique morphology that enhances the surface area and increases active sites for molecular interactions. Additionally, the nanosheets could exhibit impressive self-assembly capabilities, allowing the formation of complex structures useful for superhydrophobic surfaces. We developed Northern Tooth-like ZnO nanosheets on SS mesh by simply immersing the mesh in a solution of zinc acetate dihydrate and diethanolamine. This step was followed by a surface modification using STA to achieve superhydrophobic/superoleophilic characteristics. The modified SS mesh exhibited high efficiency in oil-water separation and permeation flux, which were evaluated using a custom-made setup. Furthermore, the mesh displayed sustainable superhydrophobicity across various tests, including the adhesive tape test, sandpaper abrasion test, and exposure to heat, as well as acidic and alkaline environments. It also remained resilient under mechanical stress, successfully enduring bending, twisting, and folding tests.

2. Experimental

2.1. Materials

Zinc acetate dihydrate [$(CH_3COO)_2Zn{\cdot}2H_2O$] was purchased from Spectrochem Pvt. Ltd., India. Diethanolamine [$(CH_2(OH)CH_2)_2NH$] and isopropyl alcohol [$(CH_2(OH)CH_2)_2NH$] were obtained from Thomas Baker Pvt. Ltd., India. Stearic acid [$CH_3(CH_2)_{16}$ COOH] was purchased from Sigma Aldrich, USA. Ethanol [C_2H_5OH] was bought from Qualikems Fine Chem Pvt. Ltd., India. Stainless steel (SS) meshes with a pore size of approximately 50 μm was obtained from Shanghai Titan Technology Co. Ltd. China. Petrol, diesel, kerosene (Bharat Petroleum Corporation Limited, India), vegetable oil (Garud, India), and coconut oil (Parachute Advanced, India) were obtained from different sources.

2.2. 2D ZnO nanosheets growth on SS mesh and superhydrophobic modification

To grow northern tooth-like nanosheets on SS mesh, we first cut the mesh into 2 × 2 cm^2 pieces and cleaned them ultrasonically in distilled water followed by ethanol for 30 min each. After cleaning, the SS mesh was dried in oven at 80 °C for 30 min. A precursor solution was prepared by dissolving 1 g of zinc acetate dihydrate in 50 mL of isopropyl alcohol, followed by stirring at room temperature for 1 h. Then, 250 μL of diethanolamine was gradually added to precursor solution, and the mixture was further stirred at 60 °C for 1 h to ensure homogeneity. After allowing the solution to age overnight for hydrolysis and condensation reactions, the cleaned SS mesh was immersed in the above-prepared solution for 1 min. The mesh was removed and dried in an oven at 100 °C for 1 h. The immersion and drying steps were repeated five times to attain uniform surface coverage of nanosheets. The processed SS mesh was subsequently immersed in a STA solution for 5 h, ethanol-washed and dried at room temperature. The STA solution was prepared by dissolving 1.25 g of STA in 50 mL of ethanol using a magnetic stirrer for 1 h. The process was repeated with different concentrations of zinc acetate dihydrate (1, 2 and 3 g) and the samples were labelled as ZnSA-1, ZnSA-2, and ZnSA-3, respectively. We observed precipitation formation at higher concentration of zinc acetate dihydrate (4 g) as the solution was kept overnight to age, indicating instability at higher concentrations (Fig. S1). A schematic of the entire process of fabrication of superhydrophobic SS mesh is illustrated in Fig. 1.

2.3. Characterization

The surface morphology of the treated SS mesh was studied using Scanning Electron Microscopy (SEM, JEOL, JSM7610F, Tokyo, Japan) and elemental composition by Energy Dispersive Spectroscopy (EDS, Hitachi, Tokyo, Japan). The water contact angle (WCA) and sliding angle of the prepared samples were measured by a contact angle meter (HO-IAD-CAM-01, Holmarc Opto-Mechatronics Pvt. Ltd., India). The surface roughness of uncoated and coated meshes was measured by Stylus profiler (Mitutoyo, SJ 210, Japan). The mechanical stability of the treated mesh was assessed through several tests, including adhesive tape peeling, sandpaper abrasion, multiple folding, bending, and twisting. For the adhesive tape peeling test, tape with an adhesive strength of 3.93 N/10 mm was used, while 320-grit sandpaper was utilized for the sandpaper abrasion test. To evaluate the thermal stability, the treated mesh was heated to 200 °C for 1 h, and the WCA was measured before and after the heat treatment. For the self-cleaning application, 5 g of fine dirt particles were mixed with 20 mL of water and poured onto an angled superhydrophobic mesh.

2.4. Oil–water separation experiments

The superhydrophobic mesh's separation capacity and permeation flux were examined using a home-designed oil-water separator. In a

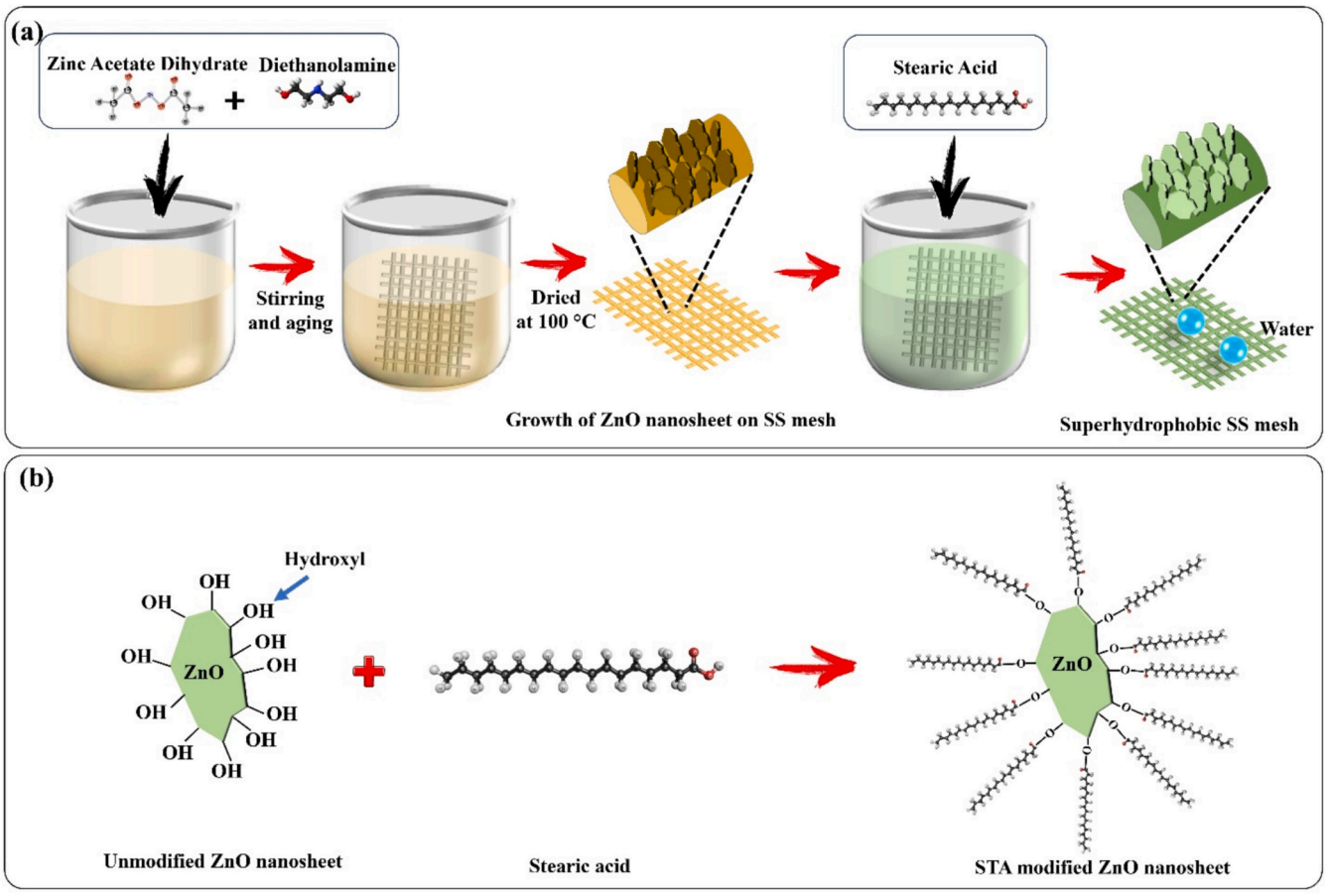

Fig. 1. Schematic diagrams of (a) growth of ZnO nanosheets on SS mesh and superhydrophobic modification, and (b) likely interaction between STA and ZnO nanosheet.

typical experiment, 10 mL of oil was added to 10 mL of water to prepare the oil-water mixture. Different viscosity oils, including petrol, diesel, kerosene, coconut, and vegetable oils were used to prepare different oil-water mixtures. The separation efficiency was calculated using Eq. (1) [28].

$$\eta = \frac{W_1}{W_0} \times 100\% \tag{1}$$

where W_0 and W_1 are the masses of the water phase before and after the separation process, respectively.

The oil permeation flux was calculated using Eq. (2) [29].

$$F = \frac{V}{At} \tag{2}$$

where V is the volume of the permeable oil phase, A is the effective separation area of the membrane during separation, and t is the total time.

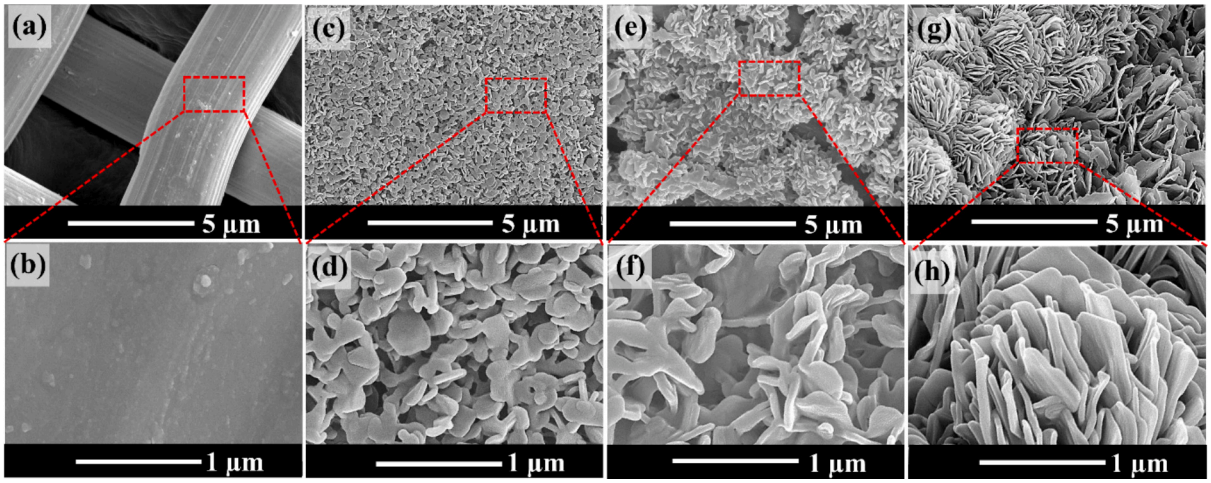

Fig. 2. FE-SEM images of (a–b) pristine SS mesh, (c-d) ZnSA-1 (e-f) ZnSA-2 and (g–h) ZnSA-3.

3. Results and discussion

3.1. Morphological and chemical properties of treated SS mesh

Surface morphology significantly influences the wettability characteristics of the solid surface. SEM images of the pristine SS mesh feature smooth SS wires with an average diameter of about 3 μm and a porous network, with pore sizes ranging from 3 μm × 4 μm (Fig. 2a). Fig. 2b highlights the relatively smooth surface of the pristine mesh wires, which is crucial for the growth of ZnO nanostructures. After the treatment, the SS mesh exhibited significant morphological changes due to the growth of ZnO nanosheets (Fig. 2c-h). At a lower concentration of zinc acetate dihydrate (1 g), as shown in Fig. 2c and d, the random growth of ZnO nanosheets exhibited vertical and horizontal orientations. Increasing the concentration to 2 g facilitated a small bunch of more vertically aligned nanosheets (Fig. 2e and f). A subsequent increase to 3 g of zinc acetate dihydrate achieved a comprehensive vertical alignment of nanosheets in bunches, exhibiting a structural resemblance to the Northern Tooth (Fig. 2g and h). The mean nanodiameter values of ZnSA-1, ZnSA-2, and ZnSA-3, as measured from SEM images using ImageJ software, were 220.04 nm, 210.91 nm, and 229.51 nm, respectively. Furthermore, the surface roughness values of the raw mesh, ZnSA-1, ZnSA-2, and ZnSA-3 were determined to be 7.88 μm, 7.38 μm, 7.55 μm, and 8.12 μm, respectively (Fig. S2). This shift in surface morphology illustrates how varying zinc acetate concentrations can significantly affect the arrangement of nanosheets and, in turn, the wettability properties of the treated SS mesh. The unique Northern Tooth-like morphology of ZnO nanosheets could enhance surface area and increase active sites for molecular interactions. Hierarchical structures significantly enhance hydrophobicity, crucial for oil-water separation [30–32]. Similarly, Northern Tooth-like ZnO morphology on SS mesh achieves superhydrophobicity through micro-scale tooth-like projections. This structure traps air pockets, significantly reducing liquid adhesion on Northern Tooth-like structures. The growth of these nanosheets involved multiple steps: firstly, the overnight aging of the precursor solution facilitated the nucleation of nanocrystals suitable for the formation of well-defined structured nanosheets [26,33–36]. The optimum zinc acetate concentration and the intermittent heating of the mesh could have favoured the vertical growth and self-assembly of nanocrystals, creating the Northern Tooth -like structure. Their vertical alignment showcases self-assembly capabilities, facilitating the creation of complex structures ideal for superhydrophobic surface design. The EDS spectra identified four key elements: carbon (C), oxygen (O), zinc (Zn), and silicon (Si). Table S1 provides the mass percentages of these elements related to different concentrations of zinc acetate dihydrate in the coating formulation.

3.2. Surface wettability

A distinctive surface-wetting property of porous materials towards water and oil significantly impacts the efficiency of separating oil-water mixtures. In this context, the performance of treated SS mesh was systematically evaluated by measuring WCAs and oil contact angles (OCAs). Typically, superhydrophobic surfaces have high WCAs and low sliding angles (SAs), enhancing water repellence while attracting oil contaminants due to altered surface polarity, resulting in superoleophilic property. The untreated SS mesh exhibited a WCA of 84° and an OCA of 22°, reflecting the influence of hydroxyl groups present on the surface, along with the inherent smoothness of the SS mesh. The surface of the unmodified ZnO nanosheet is hydrophilic due to its numerous hydroxyl groups. STA consists of a non-polar, hydrophobic alkane long chain composed of 18 carbon unsaturated hydrocarbon groups with no branching. When ZnO nanosheet-coated SS mesh immersed in STA solution, the carboxyl groups (-COOH) of STA could react and undergo esterification with the hydroxyl groups (-OH) present on the surface of ZnO nanosheets [37]. This chemical modification results in converting ZnO nanosheets from hydrophilic to superhydrophobic, as shown in Fig. 1(b). The long hydrocarbon chains (C18) of STA, which are non-polar, significantly reduce the surface energy of the ZnO nanosheet surface, enhancing its affinity for non-polar substances such as oils. However, upon growth of ZnO nanosheets and modifying the surface with STA, there was a remarkable transformation in the characteristics of the SS mesh. The relatively smooth surface underwent a roughening process with low surface energy, significantly enhancing the hydrophobic properties. We calculated the surface tension (surface energy) of the coated SS mesh using Eq. (4) [38]:

$$cos\ \theta_o = \frac{W_{SL}}{\gamma_{LA}} - 1 \tag{3}$$

$$W_{SL} = \gamma_{LA}(1 + cos\ \theta_o) \tag{4}$$

where, θ_o is the static contact angle, W_{SL} is the work of adhesion per unit area between two surfaces and γ_{LA} is the surface energy (surface tension) of the liquid against air. The calculated surface energy of ZnSA-3 was 3.56 mN/m, while for the raw SS mesh, it was 79.52 mN/m. We also calculated the solid-liquid fraction (f_{SL}) using the Eq. (5). The obtained solid-liquid fraction value for ZnSA-3 was 2.1789.

$$\text{Cos}\ \theta_{CB} = 1 + f_{SL}\ (\text{Cos}\ \theta_o - 1) \tag{5}$$

The shift in the orientation of ZnO nanosheets from a horizontal arrangement to a vertical alignment, resulting from an increase in the concentration of zinc acetate dihydrate, led to the formation of a hierarchical architecture. This configuration established unique nano- and micro-scale interspaces between neighbouring nanosheets, which demonstrated a WCA of 162 ± 2° and a SA of 3°. Conversely, oil droplets showed complete absorption, resulting in an OCA of 0°. Such inverse wettability of treated SS mesh towards water and oil could greatly influence the separation of oil-water mixtures. This study, hence, provides clear evidence that the wetting behaviour of SS mesh is profoundly altered through the growth of ZnO nanosheets, correlating positively with the increasing concentration of zinc acetate dihydrate during the synthesis process (Fig. 3a). Fig. 3b depicts the spherical water droplets resting on the ZnSA-3 sample, with a strong absorption of oil droplets, further representing the effectiveness of the modified mesh.

A notable feature of superhydrophobic coatings is their ability to self-clean [39], as demonstrated by the ZnSA-3 sample. In this test, charcoal dust was sprinkled over the ZnSA-3 coating, and when water was applied, droplets rolled off the surface, effectively collecting and removing the dust, resulting in a clean surface (Fig. 3c). Furthermore, when muddy water was poured onto a slanted ZnSA-3 sample, the droplets rolled off without leaving any residue (Fig. 3c). This illustrates the exceptional self-cleaning properties of superhydrophobic coatings, making them highly valuable for outdoor applications where maintenance is crucial.

3.3. Mechanical and environmental stability

Superhydrophobic coatings are notable for their water-repellent properties but often struggle with mechanical stability and durability in practical applications. To assess their structural integrity, we tested the mechanical strength by simulating real-world conditions through bending, folding, and twisting [40]. The superhydrophobic mesh exhibited remarkable stability after rigorous mechanical deformations like folding, bending, and twisting. This resilience confirms its suitability for dynamic applications that involve repeated or extreme distortions. Experiments simulating real-world stress conditions showed that the mesh retained its superhydrophobic properties despite these challenges, highlighting its robustness and versatility. Visual references in Fig. 4(a and b) demonstrate the coated mesh's unique properties after significant physical manipulation, emphasising its utility in demanding environments.

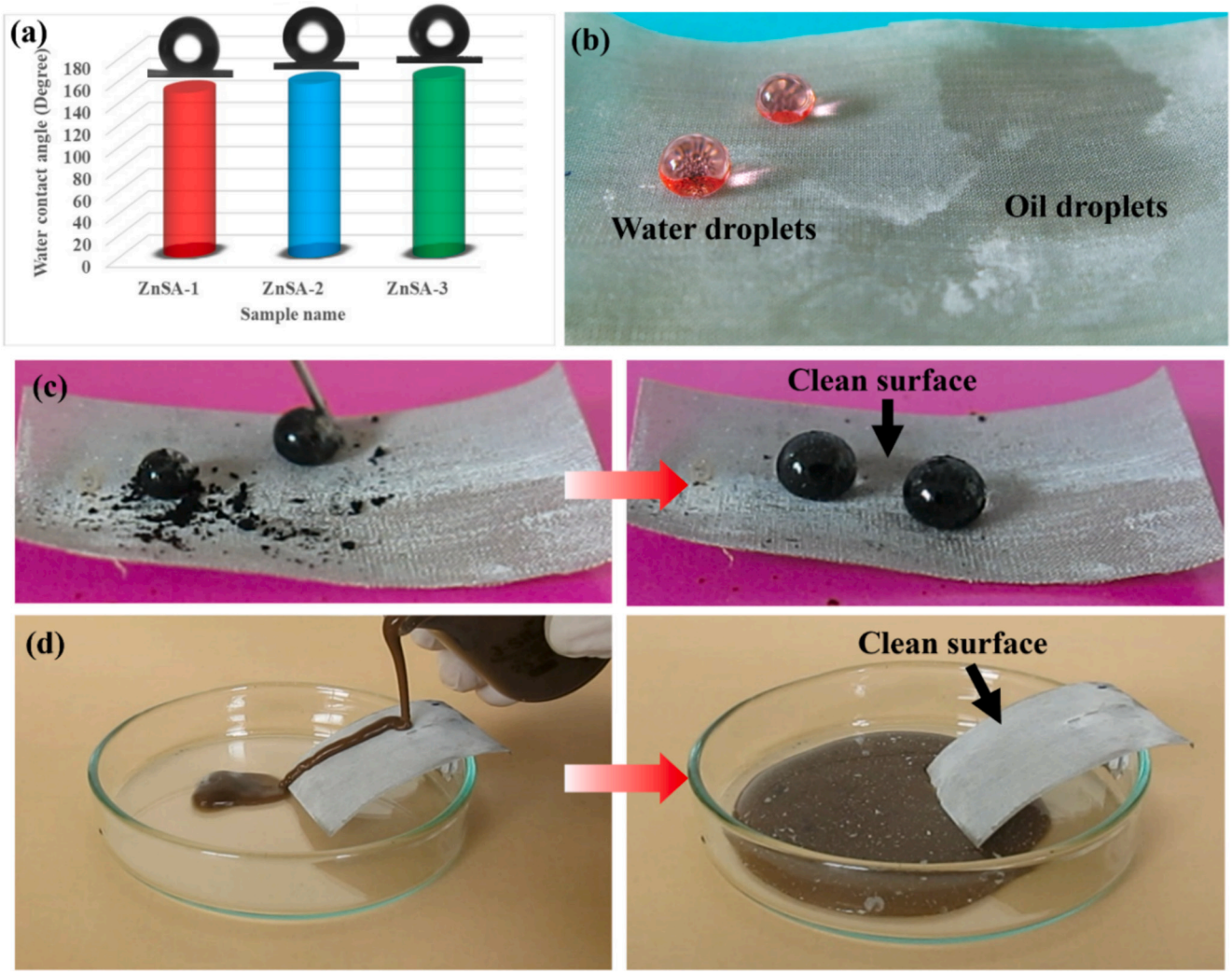

Fig. 3. (a) The variation of WCA with concentration of zinc acetate dihydrate. (b) Colour dyed water droplets and petrol droplets on ZnSA-3 sample. The screen snaps of process of self-cleaning performance of ZnSA-3 sample against (c) charcoal dust and (d) muddy water.

The chemical durability of the ZnSA-3 coating was evaluated by exposing the surface to alkaline and acidic droplets. The results showed that regardless of pH level, droplets formed distinct spherical shapes on the coated mesh (Fig. 4c). This indicates that the coating effectively resists corrosive liquids, preserving the integrity of the mesh. To evaluate the thermal stability of the samples, we subjected them to controlled heating at 200 °C for 1 h. This assessment aimed to determine how high temperatures affect coating performance. After heat treatment, the WCA decreased from 162° to 155°, indicating strong thermal stability. Fig. 4(d) shows a photograph of the heat-treated ZnSA-3 sample that reveals water droplets retaining a spherical shape, confirming the coating's superhydrophobic properties. These findings demonstrate that the superhydrophobic coating on SS mesh remains stable and durable under high-temperature conditions.

Further, we evaluated their resistance to peeling forces using adhesive tape and assessed wear with sandpaper abrasion tests [41]. To understand the impact of mechanical stress on hydrophobic properties, we investigated the variation of the WCA after these tests, aiming to clarify the relationship between mechanical stress and the long-term performance of superhydrophobic surfaces. To evaluate the mechanical stability, we performed an adhesive tape test using tape with an adhesion value of 3.93 N/10 mm. The tape was applied to the ZnSA-3 sample with a 200 g weighted disc to ensure good adhesion, and peeled it off for 70 cycles; WCA was measured after every 10 cycles. The results, shown in Fig. 4(e), indicate that the ZnSA-3 coating maintained remarkable mechanical stability, retaining a high contact angle of 154° even after 70 peeling cycles. A comprehensive sandpaper abrasion test was conducted to assess the durability and sustainability of superhydrophobic surfaces in harsh environmental conditions, as documented by Varshney et al. [42]. In this test, a ZnSA-3 sample was placed on sandpaper with a 50 g weight on top, followed by a linear pull of 15 cm for 1 cycle. To evaluate the impact of abrasion on the superhydrophobic properties of the coating, the change in WCAs was meticulously measured after every five abrasion cycles. The findings, illustrated in Fig. 4(f), indicated that the coating successfully retained its superhydrophobicity, exhibiting a WCA of 151 ± 2° even after enduring 20 complete cycles. These results underscore the impressive durability of the superhydrophobic coating, demonstrating that it retains its functional properties despite undergoing significant mechanical stress and wear.

3.4. Oil-water separation performance

The primary challenge in using superhydrophobic meshes for gravity-driven oil-water separation is their incompatibility with different types of oils. Superhydrophobic meshes work well for heavy oils but are ineffective for light oils due to water layer formation that hinders oil penetration. Increased oil-water mixture volumes can also

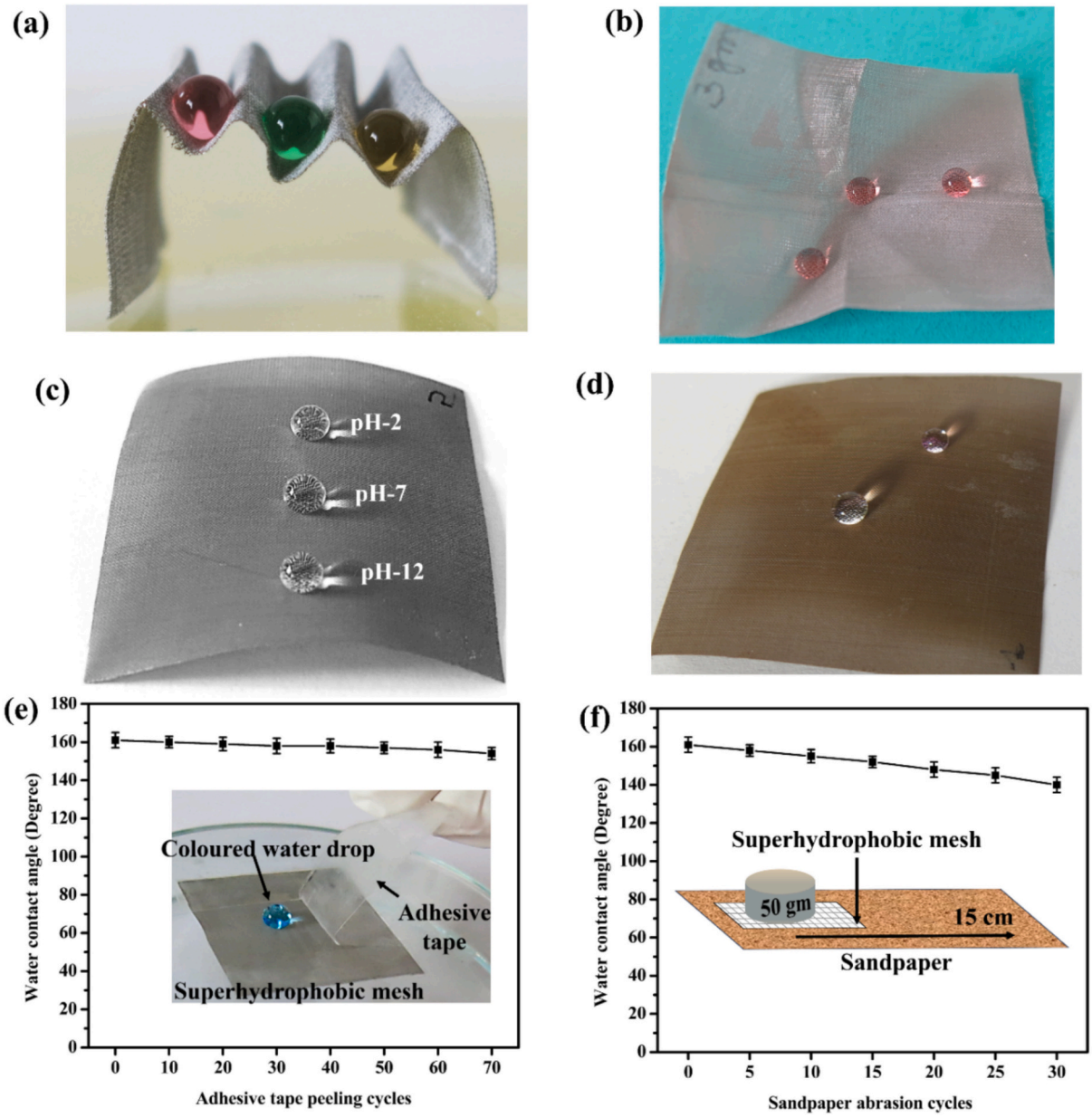

Fig. 4. (a-b) Photographs of water droplets on ZnSA-3 sample after rigorous mechanical deformations. (c) Photograph of alkaline, neutral and acidic solution droplets on the sample. (d) The droplet on sample after heating, (e, f) the variation in WCA with (e) adhesive tape peeling cycles and (f) sandpaper abrasion cycles (inset: photographs of experimental setup).

cause pressure buildup, risk of breakdown and compromising the separation process. To address these issues, it is essential to periodically remove the non-wetting liquid accumulating on the mesh, highlighting the uselessness of continuous operations in dead-end setups.

To overcome this challenge, the sieve separators offer a practical alternative, influencing gravity to separate oil and water more effectively. They are cost-effective, energy-efficient, and designed to selectively absorb oil while repelling water, allowing gentle handling of mixtures. Moreover, sieve separators are scalable for various operations and have a long lifespan with low maintenance needs, making them a robust solution for oil-water separation challenges encountered with traditional filtration methods. The innovative use of sieve separators enabled gravity separation of oil-water mixtures using our specially engineered superhydrophobic/superoleophilic ZnSA-3 coated mesh (Fig. 5a). This mesh is crafted into a mini boat design with one open end over two beakers placed at different heights. The open end of the boat is oriented towards the beaker kept at the lower height, which has a slight slope designed to encourage the movement of water droplets on the superhydrophobic mesh surface. As the water droplets roll towards the lower beaker due to gravity, oil droplets are effectively absorbed by the superoleophilic surface of the boat, allowing for efficient separation of the oil from the water.

Fig. 5(b) illustrates the screen snaps of the continuous separation of the petrol-water mixture. When a petrol-water mixture is poured onto the separator, the petrol quickly gets absorbed by the ZnSA-3 mesh, facilitating effective separation. The petrol passes through the mesh and collects in a beaker positioned below. Once all the petrol is absorbed, the remaining water droplets on the superhydrophobic mesh roll off into another beaker placed at the open end of boat. This setup efficiently collects the oil and water, demonstrating the effectiveness of the separation process. Further investigated the separation performance of the ZnSA-3 sample using various oils such as diesel, kerosene, coconut oil, and vegetable oil. The separation efficiencies and permeation fluxes were measured for different oil-water mixtures (Fig. 5c). The separation

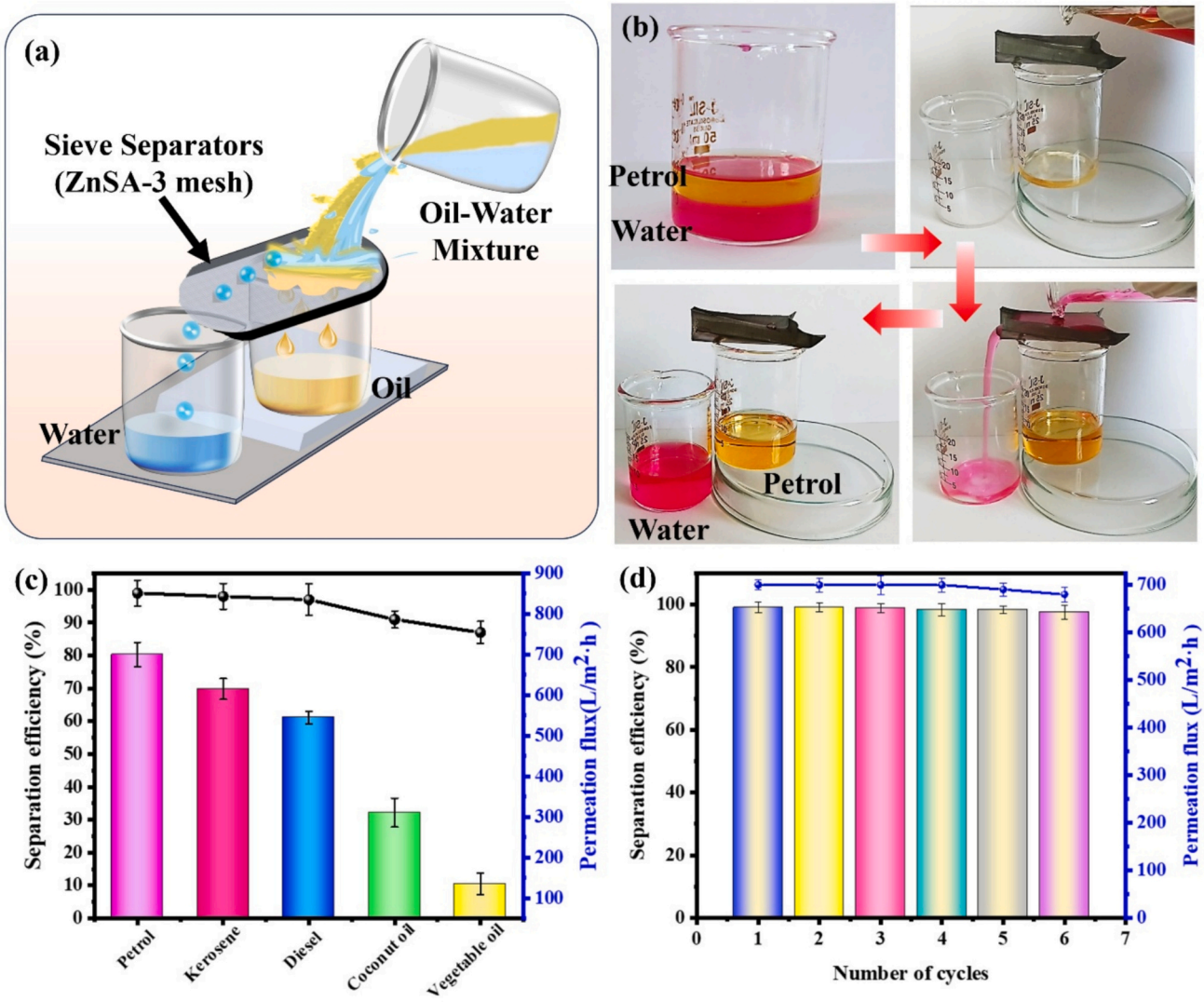

Fig. 5. (a) Schematic of oil-water mixture separation using sieve separator (ZnSA-3 mesh). (b) The screen snaps of the oil-water separation process. (c) The separation efficiencies and permeation fluxes for different oil-water mixtures. (d) The variation of separation efficiencies and permeation fluxes for petrol-water mixture during repeated cycles of separation.

Table 1
A comparison of the oil-water separation performance of various innovative surface morphologies created by ZnO nanomaterial.

Materials	Method	Innovative surface morphologies	Separation efficiency (%)	Permeation flux/oil flux (L/m^2·h)	Reusability (cycles)	WCA (°)	Ref.
ZnO particles, chitosan, sodium phytate, stearic acid	Layer-by-layer (LBL) assembly	Flower	86	–	5	156	[43]
ZnO particles, epoxy resin, stearic acid, PU sponge	Simple immersion method	Honeycomb	98	–	10	156 ± 3	[44]
Zinc acetate dihydrate, stearic acid, sodium hydroxide, cotton fabric	Plasma treatment followed by wet chemical reaction	Honeycomb	90	3531	–	151	[36]
Zinc acetate dihydrate, polyacrylonitrile, carbon nanofiber membrane	Electrospinning and dip coating	Nanorods	99.7	3531	15	163.5	[27]
ZnO particles, epoxy resin, stearic acid, SS mesh	Immersion	Petal	97	–	75	163.8	[45]
Zinc acetate, zinc (II) nitrate hexahydrate, SS mesh	Chemical bath deposition	Micro-flower with nano-needle	99	4200	10	160.1	[46]
Zinc nitrate hexahydrate, zinc acetate dihydrate, and SIC membranes	Chemical bath deposition	Nanorod, Petal	99	1300	–	172.8	[26]
Zinc nitrate, steric acid, cotton fabric	Dip-coating	Nanosheets, flowers	99.8	1515	15	162	[47]
Zinc acetate dihydrate, steric acid, SS mesh	Dip-coating	Nanosheet, northern tooth	99	700 ± 50	15	162	This work

efficiency and permeation flux of oil-water mixtures are significantly affected by the oils' viscosities. In experiments with a low-viscosity petrol-water mixture, separation efficiency reached 99 % with a permeation flux of 700.28 L/m^2·h, demonstrating effective separation. Conversely, a high-viscosity vegetable oil-water mixture exhibited only 92 % efficiency and a flux of 135 ± 50 L/m^2·h, highlighting the challenges of separating higher viscous fluids. The decline in performance underscores the difficulties associated with using highly viscous oils, indicating that viscosity is a key factor in the separation. To further investigate the separation stability, a series of repeated separations were conducted. A low-viscosity petrol-water mixture was utilized for these tests, serving as an ideal medium to evaluate separation efficiency and permeation flux. As shown in Fig. 5(d), the results demonstrated that the superhydrophobic ZnSA-3 mesh maintained consistent separation efficiency and permeation flux over multiple cycles. The results suggest that the specially designed superhydrophobic/superoleophobic ZnSA-3 mesh exhibits remarkable resilience and reliability during repeated oil-water separation tasks, suitable for practical applications.

This research highlights the advantages of a novel ZnO nanostructure, resembling Northern Tooth formations, which we compared to existing literature on superhydrophobic ZnO nanostructures, as shown in Table 1. Previous studies have explored various configurations like flower-like formations, petal structures, and nanosheets, all effective in oil-water separation. Our Northern Tooth-like structure enhances oil absorption from mixtures, improving separation efficiency due to its unique morphology that maximizes surface area interaction with oil. This advancement could lead to improved applications in wastewater treatment and separation technologies.

To demonstrate the practical applicability of our material, we have conducted comprehensive oil/water separation experiments using various complex oil/water mixtures, including petrol - 0.1 M NaCl, petrol - 0.1 M HCl, petrol - 0.1 M NaOH, and petrol-muddy water mixtures, as illustrated in Fig. S3. Furthermore, we have systematically evaluated the separation efficiency and permeation flux, as shown in Fig. S4. These findings confirm the potential of our material for real-world oily wastewater treatment applications.

4. Conclusions

We have successfully synthesized Northern tooth-like ZnO nanosheets on stainless steel mesh using a simple immersion approach, followed by a superhydrophobic surface modification for effective oil-water separation. The unique morphology enhanced surface area and oil absorption while repelling water, achieving a WCA of 162 ± 2° and an OCA of 0°. A low-viscosity petrol-water mixture showed 99 % separation efficiency with a permeation flux of 700.28 L/m^2·h, while a high-viscosity vegetable oil-water mixture achieved 92 % efficiency with a flux of 135 ± 50 L/m^2·h. The calculated surface energy of the modified mesh (3.56 mN/m) was significantly lower than the raw mesh (79.52 mN/m), contributing to its enhanced superhydrophobicity. The solid-liquid fraction of the modified surface was determined to be 2.1789, further confirming its optimized surface characteristics. The mesh retained its superhydrophobic properties even after rigorous tests, including tape peeling, sandpaper abrasion, and mechanical stress, and demonstrated resilience against heat and acidic/alkaline environments. This formulation shows significant potential for sustainable oil-water separation applications. Our comprehensive oil/water separation experiments performed using various complex oil/water mixtures support the applicability of the developed mesh for real-world wastewater treatment applications.

CRediT authorship contribution statement

Tanuja A. Ekunde: Writing – original draft, Methodology, Investigation, Conceptualization. **Pradip P. Gaikwad:** Writing – original draft, Methodology, Investigation, Conceptualization. **Rajaram S. Sutar:** Writing – original draft, Methodology, Investigation, Conceptualization. **Shrutika S. Kshirsagar:** Writing – original draft, Methodology, Investigation, Conceptualization. **Rutuja A. Ekunde:** Methodology, Data curation. **Arvind M. Yelpale:** Writing – review & editing, Validation. **Xuesong Huang:** Writing – review & editing, Validation. **Viswanathan S. Saji:** Writing – review & editing, Validation. **Shanhu Liu:** Writing – review & editing, Supervision, Funding acquisition. **Sanjay S. Latthe:** Writing – review & editing, Supervision, Project administration, Funding acquisition.

Declaration of competing interest

The authors declare that they have no known competing financial interests or personal relationships that could have appeared to influence the work reported in this paper.

Acknowledgements

One of the authors, SSL is grateful for financial assistance received through Seed Money Scheme from Vivekanand College, Kolhapur (Empowered Autonomous) 416 003, Maharashtra, India Ref. No. VCK/3108/2023-24 dated 30/03/2024.

Appendix A. Supplementary data

Supplementary data to this article can be found online at https://doi.org/10.1016/j.jwpe.2025.107368.

Data availability

Data will be made available on request.

References

[1] S. Cheng, E. He, R.S. Sutar, B. Shi, R. Xing, S. Liu, Superhydrophobic absorbent based on multiwall carbon nanotubes and superlight clay for solar-assisted crude oil cleanup, ACS Appl. Nano Mater. 7 (18) (2024) 21825–21832, https://doi.org/10.1021/acsanm.4c03795.

[2] M.I. Hasan, S. Aggarwal, Unraveling the roles of temperature, salinity, and herder volume on environmental partitioning and efficiency of OP-40 herder during in situ burning of oil spills, ACS ES&T Water 4 (4) (2024) 1403–1410, https://doi.org/10.1021/acsestwater.3c00556.

[3] S. Sankhla, S. Neogi, Ambient-dried, scalable and biodegradable cellulose nanofibers aerogel for oil-spill cleanup, J. Environ. Chem. Eng. 12 (3) (2024) 112745, https://doi.org/10.1016/j.jece.2024.112745.

[4] S. Wu, A. Mashhadian, R. Jian, S. Tian, T. Luo, G. Xiong, Designing interconnected passages by "legs-to-head" directional U-shape freeze casting to boost solar-driven self-pumping oil spill recovery, J. Mater. Chem. A 12 (21) (2024) 12866–12875, https://doi.org/10.1039/D3TA07164B.

[5] C. Fu, G. Tian, S. He, L. Yao, Z. Guo, Hydrogel coated mesh with controlled flux for oil/water separation, ACS Appl. Mater. Interfaces 16 (29) (2024) 37757–37769, https://doi.org/10.1021/acsami.4c08781.

[6] X. Yan, Y. Wang, Z. Huang, Z. Gao, X. Mao, M.J. Kipper, L. Huang, J. Tang, Janus polyacrylonitrile/carbon nanotube nanofiber membranes for oil/water separation, ACS Appl. Nano Mater. 6 (6) (2023) 4511–4521, https://doi.org/10.1021/acsanm.3c00006.

[7] Y. Pan, Z. Zhu, M. Li, Y. Chen, C. Cheng, M. Wang, H. Sun, A. Li, Preparation of halloysite-based superhydrophobic aerogels for oil–water separation, ACS Appl. Polym. Mater. 6 (17) (2024) 10842–10852, https://doi.org/10.1021/acsapm.4c01976.

[8] Z. Deng, K. Lv, G. Zhu, X. Zhao, Y. Feng, Superhydrophobic sponge for highly efficient separation of both stratified and emulsified oil–water mixtures, Ind. Eng. Chem. Res. 62 (25) (2023) 9714–9725, https://doi.org/10.1021/acs.iecr.3c00899.

[9] J.-Y. Wang, Z.-M. Xiong, L. Guo, Y.-F. Zhang, F. Zhang, F.-P. Du, Enhanced superhydrophobicity and durability of modified cotton cloth for efficient oil-water separation, Sep. Purif. Technol. 354 (2025) 128716, https://doi.org/10.1016/j.seppur.2024.128716.

[10] Y. Liu, S. Cheng, S.K. Kannan, P. Zhang, R.S. Sutar, B. Shi, S. Liu, Scalable superhydrophobic CB/PVFM sponge for enhanced cleanup of crude oil exploiting photothermal and electrothermal effects, ACS Appl. Polym. Mater. 6 (14) (2024) 8367–8376, https://doi.org/10.1021/acsapm.4c01204.

[11] X. Yin, S. Yu, L. Wang, H. Li, W. Xiong, Design and preparation of superhydrophobic NiS nanorods on Ni mesh for oil-water separation, Sep. Purif. Technol. 234 (2020) 116126, https://doi.org/10.1016/j.seppur.2019.116126.

[12] F. Hassani, A. Aroujalian, A. Rashidi, Development of superhydrophobic and superoleophilic CNT and BNNT coated copper meshes for oil/water separation, Sci. Rep. 14 (1) (2024) 14706, https://doi.org/10.1038/s41598-024-65414-5.
[13] Z. Xu, D. Jiang, Z. Wei, J. Chen, J. Jing, Fabrication of superhydrophobic nano-aluminum films on stainless steel meshes by electrophoretic deposition for oil-water separation, Appl. Surf. Sci. 427 (2018) 253–261, https://doi.org/10.1016/j.apsusc.2017.08.189.
[14] J. Wang, X. Wang, S. Zhao, B. Sun, Z. Wang, J. Wang, Robust superhydrophobic mesh coated by PANI/TiO2 nanoclusters for oil/water separation with high flux, self-cleaning, photodegradation and anti-corrosion, Sep. Purif. Technol. 235 (2020) 116166, https://doi.org/10.1016/j.seppur.2019.116166.
[15] P. Fang, L. Huang, W. Pan, S. Wu, X. Feng, J. Song, Y. Xing, Facile preparation of durable superhydrophobic-superoleophilic mesh using simple chemical oxidation for oil-water separation under harsh conditions, Colloids Surf. A Physicochem. Eng. Asp. 624 (2021) 126777, https://doi.org/10.1016/j.colsurfa.2021.126777.
[16] P. Raturi, K. Yadav, J. Singh, ZnO-nanowires-coated smart surface mesh with reversible wettability for efficient on-demand oil/water separation, ACS Appl. Mater. Interfaces 9 (7) (2017) 6007–6013, https://doi.org/10.1021/acsami.6b14448.
[17] M.I. Rahmah, R.S. Sabry, W.J. Aziz, Preparation of superhydrophobic Ag/Fe_2O_3/ZnO surfaces with photocatalytic activity, Surf. Eng. 37 (2021) 1320–1327, https://doi.org/10.1080/02670844.2021.1948156.
[18] Z.-X. Yang, L.-C. Jing, X. Ming, W.-H. Geng, W. Cao, Y. Tian, P.-S. Bin, Z.-L. Bao, R.-Y. Chang, H.-Z. Geng, Preparation and performance study of superhydrophobic layer based on fluffy ZnO rods/PDMS, Surfaces and Interfaces 39 (2023) 102968, https://doi.org/10.1016/j.surfin.2023.102968.
[19] R. Li, M. Li, X. Wu, H. Yu, R. Jin, J. Liang, **A** pine needle-like superhydrophobic Zn/ZnO coating with excellent mechanochemical robustness and corrosion resistance, Mater. Des. 225 (2023) 111583, https://doi.org/10.1016/j.matdes.2022.111583.
[20] J. Xu, K. Guan, P. Luo, S. He, H. Matsuyama, D. Zou, Z. Zhong, Engineering PVDF omniphobic membranes with flower-like micro-nano structures for robust membrane distillation, Desalination 578 (2024) 117442, https://doi.org/10.1016/j.desal.2024.117442.
[21] Y. Xie, P. Tu, Y. Xiao, X. Li, M. Ren, Z. Cai, B. Xu, Designing non-fluorinated superhydrophobic fabrics with durable stability and photocatalytic functionality, ACS Appl. Mater. Interfaces 15 (33) (2023) 40011–40021, https://doi.org/10.1021/acsami.3c07352.
[22] M.I. Rahmah, R.S. Sabry, W.J. Aziz, Preparation and photocatalytic property of Fe_2O_3/ZnO composites with superhydrophobicity, Int. J. Miner. Metall. Mater. 28 (2021) 1072–1079, https://doi.org/10.1007/s12613-020-2096-y.
[23] Z. Liu, T. Zhao, W. Fan, X. Men, K. Jiang, G. Lu, A triple bioinspired surface based on perfluorodecyl trimethoxysilane-coated ZnO nanosheets for self-driven water transport in a flow channel, ACS Appl. Nano Mater. 5 (2) (2022) 2280–2292, https://doi.org/10.1021/acsanm.1c03988.
[24] Q. Xiong, Q. Tian, X. Yue, J. Xu, X. He, F. Qiu, T. Zhang, Superhydrophobic PET@ZnO nanofibrous membrane extract from waste plastic for efficient water-in-oil emulsion separation, Ind. Eng. Chem. Res. 61 (32) (2022) 11804–11814, https://doi.org/10.1021/acs.iecr.2c01742.
[25] J. Wang, Q. Du, J. Luan, X. Zhu, J. Pang, ZnO nanoneedle-modified PEEK fiber felt for improving anti-fouling performance of oil/water separation, Langmuir 37 (24) (2021) 7449–7456, https://doi.org/10.1021/acs.langmuir.1c00838.
[26] J. Wei, P. Nian, Y. Wang, X. Wang, Y. Wang, N. Xu, Y. Wei, Preparation of superhydrophobic-superoleophilic ZnO nanoflower@SiC composite ceramic membranes for water-in-oil emulsion separation, Sep. Purif. Technol. 292 (2022) 121002, https://doi.org/10.1016/j.seppur.2022.121002.
[27] L. Bai, X. Wang, X. Guo, F. Liu, H. Sun, H. Wang, J. Li, Superhydrophobic electrospun carbon nanofiber membrane decorated by surfactant-assisted in-situ growth of ZnO for oil–water separation, Appl. Surf. Sci. 622 (2023) 156938, https://doi.org/10.1016/j.apsusc.2023.156938.
[28] C. Zhao, H. Xie, H. Huang, Y. Cai, Z. Chen, J. Cheng, D. Xiang, D. Li, Z. Li, Y. Wu, Superhydrophobic/superoleophilic polystyrene-based porous material with superelasticity for highly efficient and continuous oil/water separation in harsh environments, J. Hazard. Mater. 472 (2024) 134566, https://doi.org/10.1016/j.jhazmat.2024.134566.
[29] C. Chen, D. Weng, A. Mahmood, S. Chen, J. Wang, Separation mechanism and construction of surfaces with special wettability for oil/water separation, ACS Appl. Mater. Interfaces 11 (11) (2019) 11006–11027, https://doi.org/10.1021/acsami.9b01293.
[30] P. Zhang, S. Xiang, R.R. Gonzales, Z. Li, Y.-H. Chiao, K. Guan, M. Hu, P. Xu, Z. Mai, S. Rajabzadeh, Wetting-and scaling-resistant superhydrophobic hollow fiber membrane with hierarchical surface structure for membrane distillation, J. Membr. Sci. 693 (2024) 122338, https://doi.org/10.1016/j.memsci.2023.122338.
[31] Y.C. Woo, Y. Kim, M. Yao, L.D. Tijing, J.-S. Choi, S. Lee, S.-H. Kim, H.K. Shon, Hierarchical composite membranes with robust omniphobic surface using layer-by-layer assembly technique, Environ. Sci. Technol. 52 (2018) 2186–2196, https://doi.org/10.1021/acs.est.7b05450.
[32] R. Zheng, Y. Chen, J. Wang, J. Song, X.-M. Li, T. He, Preparation of omniphobic PVDF membrane with hierarchical structure for treating saline oily wastewater using direct contact membrane distillation, J. Membr. Sci. 555 (2018) 197–205, https://doi.org/10.1016/j.memsci.2018.03.041.
[33] F.U. Ahmed, D.D. Purkayastha, Superhydrophilic ZnO nano-needle decorated over nanofibrous PAN membrane and its application towards oil/water separation, J. Environ. Chem. Eng. 11 (6) (2023) 111166, https://doi.org/10.1016/j.jece.2023.111166.
[34] I. Aier, D. Dhar Purkayastha, Hierarchical 0D CuO wrapped by petal-like 2D ZnO: a strategic approach of superhydrophobic melamine sponge toward wastewater treatment, Langmuir 40 (18) (2024) 9702–9716, https://doi.org/10.1021/acs.langmuir.4c00651.
[35] H. Peng, H. Yang, X. Ma, T. Shi, Z. Li, S. Xue, Q. Wang, In situ fabrication of flower-like ZnO on aluminum alloy surface with superhydrophobicity, Colloids Surf. A Physicochem. Eng. Asp. 643 (2022) 128800, https://doi.org/10.1016/j.colsurfa.2022.128800.
[36] C. Shi, H. Ma, Z. Wo, X. Zhang, Superhydrophobic modification of the surface of cellulosic materials based on honeycomb-like zinc oxide structures and their application in oil–water separation, Appl. Surf. Sci. 563 (2021) 150291, https://doi.org/10.1016/j.apsusc.2021.150291.
[37] R.S. Sabry, M.I. Rahmah, W.J. Aziz, A systematic study to evaluate effects of stearic acid on superhydrophobicity and photocatalytic properties of Ag-doped ZnO nanostructures, J. Mater. Sci. Mater. Electron. 31 (2020) 13382–13391, https://doi.org/10.1007/s10854-020-03893-8.
[38] B. Wang, Y. Zhang, L. Shi, J. Li, Z. Guo, Advances in the theory of superhydrophobic surfaces, J. Mater. Chem. 22 (2012) 20112–20127, https://doi.org/10.1039/C2JM32780E.
[39] A.M. Kokare, R.S. Sutar, S. Deshmukh, R. Xing, S. Liu, S.S. Latthe, ODS–modified TiO_2 nanoparticles for the preparation of self-cleaning superhydrophobic coating, in: AIP Conf. Proc, AIP Publishing, 2018, https://doi.org/10.1063/1.5033004.
[40] R.S. Sutar, S.S. Latthe, N.B. Gharge, P.P. Gaikwad, A.R. Jundle, S.S. Ingole, R. A. Ekunde, S. Nagappan, K.H. Park, A.K. Bhosale, Facile approach to fabricate a high-performance superhydrophobic PS/OTS modified SS mesh for oil-water separation, Colloids Surf. A Physicochem. Eng. Asp. 657 (2023) 130561, https://doi.org/10.1016/j.colsurfa.2022.130561.
[41] Q. Li, Y. Li, P. Xu, X. He, R. Wang, X. Zhou, Q. Liu, One-step fabrication bioinspired flexible hierarchical micro–nano structures with different morphologies, ACS Appl. Mater. Interfaces 15 (36) (2023) 43016–43025, https://doi.org/10.1021/acsami.3c09243.
[42] P. Varshney, D. Nanda, M. Satapathy, S.S. Mohapatra, A. Kumar, A facile modification of steel mesh for oil–water separation, New J. Chem. 41 (15) (2017) 7463–7471, https://doi.org/10.1039/C7NJ01265A.
[43] M. Yu, L. Yang, L. Yan, T. Wang, Y. Wang, Y. Qin, L. Xiong, R. Shi, Q. Sun, ZnO nanoparticles coated and stearic acid modified superhydrophobic chitosan film for self-cleaning and oil–water separation, Int. J. Biol. Macromol. 231 (2023) 123293, https://doi.org/10.1016/j.ijbiomac.2023.123293.
[44] R. Sun, N. Yu, J. Zhao, J. Mo, Y. Pan, D. Luo, Chemically stable superhydrophobic polyurethane sponge coated with ZnO/epoxy resin coating for effective oil/water separation, Colloids Surf. A Physicochem. Eng. Asp. 611 (2021) 125850, https://doi.org/10.1016/j.colsurfa.2020.125850.
[45] N. LorwaniSHaisarn, P. Kasemsiri, N. Srikhao, K. Jetsrisuparb, J.T. Knijnenburg, S. Hiziroglu, U. Pongsa, P. Chindaprasirt, Fabrication of durable superhydrophobic epoxy/cashew nut shell liquid based coating containing flower-like zinc oxide for continuous oil/water separation, Surf. Coat. Technol. 366 (2019) 106–113, https://doi.org/10.1016/j.surfcoat.2019.03.021.
[46] E. Velayi, R. Norouzbeigi, A mesh membrane coated with dual-scale superhydrophobic nano zinc oxide: efficient oil-water separation, Surf. Coat. Technol. 385 (2020) 125394, https://doi.org/10.1016/j.surfcoat.2020.125394.
[47] J. Wang, J. Zhang, X. Pei, S. Liu, Y. Li, C. Wang, Rapid dipping preparation of robust $Zn(OH)_2$@STA nanosheet coating on cotton fabric for multifunctional high efficient oil-water separation, Colloids Surf. A Physicochem. Eng. Asp. 598 (2020) 124868, https://doi.org/10.1016/j.colsurfa.2020.124868.